Bull. Chem. Soc. Ethiop. **2026**, 40(10), 2081-2095.
DOI: https://dx.doi.org/10.4314/bcse.v40i10.3

ISSN 1011-3924
Printed in Ethiopia
Online ISSN 1726-801X

THE USE OF ACTIVATED CARBON FOR THE REMOVAL OF FAVIPIRAVIR FROM AQUEOUS SOLUTIONS: ISOTHERM, KINETIC AND THERMODYNAMIC STUDIES

Nazan Yılmaz[1]*, Oğuzhan Alagöz[1], İbrahim Bulduk[1]

[1]Department of Chemical Engineering, Faculty of Engineering, Afyon Kocatepe University, Afyonkarahisar, Turkey

(Received January 2, 2026; Revised May 19, 2026; Accepted June 22, 2026)

ABSTRACT. This study investigates the removal of the antiviral drug favipiravir (FPR) from aqueous solutions using activated carbon through batch adsorption experiments. The effects of initial concentration, pH, adsorbent dosage, contact time, and temperature on adsorption performance were systematically evaluated. The highest FPR removal efficiency (91.93%) was achieved at an initial concentration of 30 mg/L, an adsorbent dose of 0.30 g/L, a contact time of 120 min, a temperature of 20 °C, and pH 3.0. Adsorption kinetics were analyzed using pseudo-first-order and pseudo-second-order models. The pseudo-second-order model provided the best fit (R^2 = 0.9999), indicating that the adsorption process was predominantly governed by surface interactions. Equilibrium data were evaluated using Langmuir and Freundlich isotherm models. The Langmuir model showed superior agreement with the experimental data (R^2 = 0.9982), suggesting monolayer adsorption on a homogeneous surface. Thermodynamic analysis performed at 20, 35, and 50 °C revealed negative $\Delta G°$ (-8.873 kJ mol^{-1}) and $\Delta H°$ (-29.61 kJ mol^{-1}) values, confirming that the adsorption process was spontaneous and exothermic. The negative $\Delta S°$ value (-70.77 J mol^{-1} K^{-1}) indicated decreased randomness at the solid–liquid interface. These findings demonstrate the potential of activated carbon as an effective adsorbent for the removal of favipiravir from water.

KEY WORDS: Favipiravir, Activated carbon, Batch adsorption, Water treatment, Adsorption kinetics, Thermodynamics

INTRODUCTION

Human and animal health services utilize pharmaceuticals to prolong lifespan and enhance quality of life [1,2]. In recent years, increased consumption of drugs and their release into the environment has become a global environmental problem [3]. Precise monitoring of pharmaceutical contamination of water supplies on a global scale is required [2]. Antiviral pharmaceuticals are a class of drugs that inhibit the growth of pathogens and ultimately treat viral infections [4]. Recently, increasing mortality rates due to viral infections have led to the production and consumption of ever-increasing quantities of antiviral drugs [5]. These drugs have extensive application in treating a spectrum of viral infections, including hepatitis, influenza, herpes, and human immunodeficiency virus (HIV) [4-6]. The presence of these drugs has been detected in hospital wastewater, domestic wastewater, and pharmaceutical industry wastewater [7]. Therefore, the use of antiviral drugs seriously threatens the quality of water resources intended for human consumption [8]. The unmetabolized residues of antiviral drugs are predominantly eliminated by patients through urine or faeces, ultimately entering the sewage system. Scientific investigations have indicated that up to 60% of the administered dose of antiviral drugs is excreted by patients [4,6]. Ultimately, antiviral drugs are discharged into the aquatic environment due to insufficient wastewater treatment facilities [4, 9-11].

Continuous use of drugs has led to an increase in water pollution and has led to adverse effects such as toxicity, genotoxicity in the ecosystem, endocrine disruption, and development of resistance to pathogenic microbes [1, 12]. Concurrently, the coexistence of antiviral agents and

*Corresponding author. E-mail: nazanyilmaz@aku.edu.tr

their target viruses in aquatic environments may facilitate the acquisition of drug resistance by susceptible organisms, thereby contributing to the emergence of novel antiviral resistance in these environments [13]. Favipiravir (FPR), designed as an antiviral agent targeting viral infections, belongs to the class of nucleic acid analogs. The systematic names of FPR are 6-Fluoro-3-hydroxy-2-pyrazinecarboxamide,6-fluoro-3,4-dihydro-3-oxo-2 pyrazinecarboxamide [14].

During the 2019 coronavirus pandemic, FPR demonstrated efficacy as a treatment for COVID-19, yielding positive outcomes such as elevated discharge rates and reduced necessity for mechanical ventilation [15,16]. Additionally, patients receiving FPR exhibited a notable increase in viral clearance rates within the initial two weeks of treatment [17]. The extensive utilization of FPR during influenza seasons, particularly during the COVID-19 pandemic, has precipitated a significant environmental concern due to the escalation of pharmaceutical residues across diverse water matrices [5, 13]. These pharmaceutical pollutants exhibit substantial resistance to biodegradation [18], and conventional wastewater treatment methodologies inadequately address their removal [19]. Various treatment technologies, such as the electrochemical advanced oxidation process, photolysis, photocatalysis, ozonation, membrane bioreactor, and activated sludge process, have been used to date to remove antiviral drugs from water and wastewater. While these technologies are effective in removing antiviral drugs from water sources, they have disadvantages such as high energy consumption, large equipment costs, formation of harmful by-products, and secondary contamination [20].

Adsorption emerges as a highly competitive method for pharmaceutical removal from aqueous solutions, owing to the availability of a diverse array of adsorbents, simplicity of application, and cost-effectiveness [21, 22]. Consequently, a burgeoning interest is developing in highly efficient, economical, renewable, and readily accessible adsorbents [23]. The literature review showed that there are no studies on the removal of the antiviral drug FPR from wastewater.

In this study, the adsorption method was used to remove FPR from wastewater. The parameters affecting the adsorption of FPR on activated carbon were examined in detail, and the optimum adsorption conditions were determined. Additionally, the adsorption mechanism was evaluated through isotherm and kinetic studies.

EXPERIMENTAL

Materials

Chemicals used in the study: Favipiravir (≥ 98.0%), acetonitrile (≥ 99.9%), methanol (≥ 99.0%), ethanol (≥ 99%), NaOH solution (0.1 N), HCl solution (0.1 N), H_3PO_4 (85%), KH_2PO_4 (≥ 99.0%), and activated carbon were purchased from Sigma-Aldrich Chemie (Istanbul, Turkey). The commercial activated carbon used in this study was used as received from the supplier without any additional washing or pretreatment.

An HPLC system (Agilent 1260, USA) equipped with an ultraviolet detector and Chemstation software was used to determine the concentration of FPR in aqueous solutions. A pH meter (Mettler-Toledo, Switzerland) equipped with a glass electrode was used for pH measurements. Ultrapure water used in the experimental studies was produced using a water purifier (Merck-Millipore Milli-Q, USA). Batch adsorption studies were carried out using a shaking water bath (WITEG WSB-30, Germany).

Method

Characterization of activated carbon

The surface morphology of activated carbon was characterized by scanning electron microscopy (SEM, Zeiss Sigma 300). Surface area, pore size distribution, and total pore volume of activated carbon were analyzed using a Micromeritics Gemini VII surface area analyzer.

Determination of the pHpzc value of activated carbon

The pHpzc value of activated carbon was determined through a series of steps. Initially, a 0.1 M NaCl solution was prepared. Subsequently, 50 mL aliquots of this solution were transferred into 250 mL volumetric flasks. The pH of each flask was adjusted to values of 2, 4, 6, 8, 10, and 12 using either 0.1 M HCl or 0.1 M NaOH solutions. Following pH adjustment, 0.050 g of activated carbon was added to each flask. The flasks were then placed on a shaker and agitated for a duration of 48 hours at a constant temperature of 20 °C and a shaking speed of 150 rpm. At the end of 48 hours, each mixture was filtered through white band filter paper, and the pHf values of each sample were determined with a pH meter, and the ΔpH versus pHi curve was plotted [24].

Batch adsorption experiments

Batch adsorption experiments were conducted in 250 mL capped flasks, utilizing 50 mL of the prepared FPR solutions. FPR solutions used in the experimental series were prepared at desired concentrations by dilution from the 500 mg/L stock solution. Activated carbon was previously weighed and added to the solution, and then the flasks were introduced into a shaker under a rotation of 150 rpm. Samples taken after the experiments were filtered through a 0.22 µm injector tip membrane filter, and the FPR concentrations were measured in HPLC. In the adsorption experiments, the influence of solution pH (2-12), adsorbent dose (0.2-0.6 g/L), initial concentration (25-100 mg/L), and temperature (20-50 °C) on the efficiency of FPR removal was systematically investigated. The pH of the solutions within the range of 2 to 12 was adjusted using 0.1 N HCl and 0.1 N NaOH solutions. All experiments were carried out in three replicates, and the results were averaged. The amount of FPR adsorbed per unit mass of activated carbon at the moment of t (q_t) and at the moment of equilibrium (q_e) was calculated from the following equations:

$$q_t = \left(\frac{C_0 - C_t}{w}\right) \times V \quad (1)$$

$$q_e = \left(\frac{C_0 - C_e}{w}\right) \times V \quad (2)$$

Additionally, the percentage of FPR adsorbed was calculated using the following equation:

$$\text{Removal (\%)} = \left(\frac{C_0 - C_e}{C_0}\right) \times 100 \quad (3)$$

where C_0 (mg/L) is the initial concentration, Ce (mg/L) is the equilibrium concentration, Ct (mg/L) is the concentration at time t, V (L) is the solution volume, and w (g) is the mass of activated carbon [25-27].

Adsorption isotherm modeling

Adsorption isotherms constitute a fundamental component of adsorption investigations, offering valuable insights into the physical interactions between the adsorbate and adsorbent. Through isotherm analysis, it becomes feasible to assess and characterize the nature of these interactions, thereby facilitating a comprehensive understanding of the adsorption process. The experimental curves were generated under the following conditions: initial concentration of 30 mg/L, pH adjusted to 3, adsorbent dose of 0.30 g/L, contact time of 120 minutes, and temperature at 293 K. In the present study, the equilibrium adsorption data were analyzed using the Langmuir and the Freundlich isotherm models. The experimental adsorption capacity at equilibrium (qe) was calculated using Equation (2) [25-27].

$$\frac{C_e}{q_e}=\frac{1}{q_m K_L}+\frac{C_e}{q_m} \quad (4)$$

In this equation, K_L is the Langmuir adsorption constant (L mg^{-1}), and q_m is the monolayer adsorption capacity of activated carbon (mg g^{-1}). The affinity between adsorbate and adsorbent can be determined with the help of the dimensionless separation factor (R_L). R_L is calculated by the following formula:

$$R_L=\frac{1}{1+K_L C_0} \quad (5)$$

Where C_0 is the initial adsorbate concentration of the solution (mg/L). If the R_L value is greater than 1, the isotherm shape is unfavorable. If the R_L value is equal to 1, the isotherm shape is linear. If the R_L value is between 0 and 1, the isotherm shape is favorable. If the R_L value is equal to 0, it is irreversible.

$$\ln q_e = \ln K_F + \frac{1}{n} \ln C_e \quad (6)$$

In this equation, K_F (L mg^{-1}) is the Freundlich constant and n is a parameter describing the favorability of the adsorption process; if n > 1, FPR adsorption on the adsorbent is expected to occur at high concentrations [28].

Kinetic modeling of the adsorption process

A kinetics study provides information like reaction order and rate constants, which are important factors in applying adsorption. The pseudo-first-order (Equation 7) and pseudo-second-order (Equation 8) models are commonly employed to understand the kinetics of adsorption processes.

$$\ln(q_e - q_t) = \ln q_e - k_1 t \quad (7)$$

$$\frac{t}{q_t}=\frac{1}{k_2 q_e^2}+\frac{1}{q_e} t \quad (8)$$

Where k^1 is the pseudo-first-order adsorption rate constant (1 min^{-1}), qe and qt are the adsorption capacity (mg g^{-1}) at equilibrium and time t, k_2 is the so-called second-order adsorption rate constant (g mg^{-1} min^{-1}), respectively [25, 26, 29].

Thermodynamic modeling of the adsorption process

The thermodynamic parameters ΔH° (molar enthalpy), ΔS° (molar entropy), and ΔG° (molar Gibbs energy) are crucial in understanding the energetics and spontaneity of adsorption processes. These parameters can be determined by constructing equilibrium isotherms at different temperatures and analyzing the data using thermodynamic equations. The Gibbs free energy change can be determined from the equation given below [25, 26, 30].

$$\Delta G^0 = -RT \ln K_e \quad (9)$$

In this equation, K_e is the equilibrium constant, R is the gas constant (8.314 J mol^{-1} K^{-1}), and T is the absolute temperature (K).

$$K_e=\frac{q_e}{C_e} \quad (10)$$

In this equation, C_e and q_e are the equilibrium concentration of FPR in solution (mg L^{-1}) and on the adsorbent (mg g^{-1}), respectively. The ratio qe/Ce was used as an apparent equilibrium constant

(Ke) to estimate the thermodynamic parameters and compare the adsorption behavior at different temperatures. The equation given below expresses the relationship between ΔG°, ΔH° and ΔS°:

$$\Delta G^0 = \Delta H^0 - T\,\Delta S^0 \quad (11)$$

After manipulating Equation 9, a linear equation for the calculation of thermodynamic parameters is obtained.

$$\ln K_e = -\frac{\Delta G^0}{RT} = \frac{\Delta S^0}{R} - \frac{\Delta H^0}{RT} \quad (12)$$

Analytical method and validation

An HPLC method was developed for the quantification of FPR in aqueous solutions. The conditions of the developed chromatographic method are presented below: In the chromatographic method, an ODS 3 C18 (250 mm × 4.6 mm i.d., 5 µm) column was used for separation at a constant temperature of 25 °C. The mobile phase was a 10 mM KH_2PO_4 solution (pH: 2.0 with orthophosphoric acid) and acetonitrile (70:30, V/V). Isocratic elution with a flow rate of 1.0 mL min^{-1} and eluent detection was performed at a wavelength of 227 nm using an ultraviolet detector. The developed analytical method was validated for the parameters "system suitability, specificity, linearity, precision, accuracy, robustness and sensitivity" according to ICH Q2 (R1) guidelines [31].

The linearity of the HPLC method was determined by injecting standard solutions in the concentration range 5-30 mg/L into the HPLC system on three consecutive days. The chromatographic responses (peak areas) from the instrument were recorded for each concentration of the standard solutions. A calibration curve was plotted with concentrations on the x-axis and chromatographic responses (peak areas) on the y-axis. Data from the analytical method were used for regression analysis using the least squares method. The linearity of the method was determined by the absolute mean recovery, relative standard deviation and R2 of the calibration curve. The sensitivity of the HPLC technique was assessed by determining the limits of detection (LOD) and limits of quantification (LOQ).

RESULTS AND DISCUSSION

Characterization of activated carbon

Activated carbon was characterized by BET and SEM analysis. SEM analysis was utilized to examine the surface morphology of activated carbon. When the SEM images given in Figure 1 are examined, it is seen that activated carbon has a porous structure of different sizes.

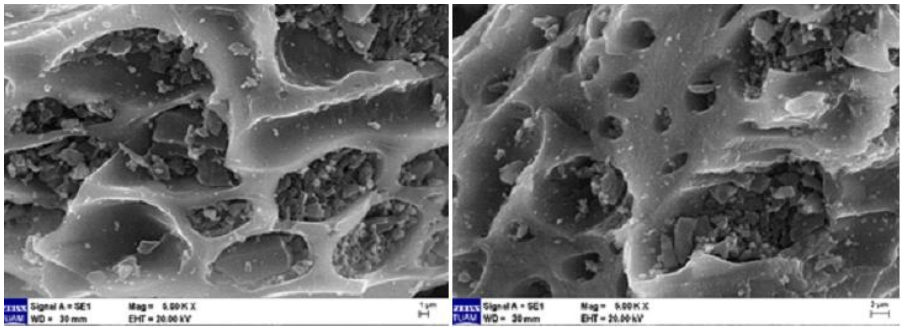

Figure 1. SEM images of activated carbon.

According to the results of the BET analysis, it was seen that the activated carbon used in the study had a surface area of 728.25 m^2/g and an average pore size of 3.13 nm and was suitable for the Type II isotherm according to the IUPAC classification. Conforming to the type II isotherm classification suggests that the activated carbon possesses specific surface characteristics and pore structures conducive to efficient adsorption processes, making it suitable for various applications such as gas purification, wastewater treatment, and solvent recovery [32].

Validation results of the analytical method

A calibration graph was created, plotting peak area values against concentration. The regression equation, slope, and intercept were computed using the least squares method of linear regression. The linearity of the method was evaluated by the absolute mean recovery, RSD and R^2 of the obtained calibration curve. The results obtained from the validation studies confirmed that the developed HPLC method was accurate, linear, sensitive, precise, and robust in accordance with ICH guidelines.

Determination of zero adsorbent charge point (pHpzc)

The zero-charge point (pHpzc) of the activated carbon, which is a crucial concept in understanding the behavior of adsorbents in solution, was determined. When the pH is lower than pHpzc, the surface functional groups of the adsorbent are protonated, resulting in a positive surface charge and making the adsorbent suitable for adsorbing anions. Conversely, when pH is higher than pHpzc, the surface is deprotonated due to the presence of OH^- ions, resulting in a negative surface charge, and the negative charge makes the adsorbent suitable for adsorbing cations [33]. The results of the experiment are presented in Figure 2, and the value of pHpzc for the adsorbent was found to be 8.

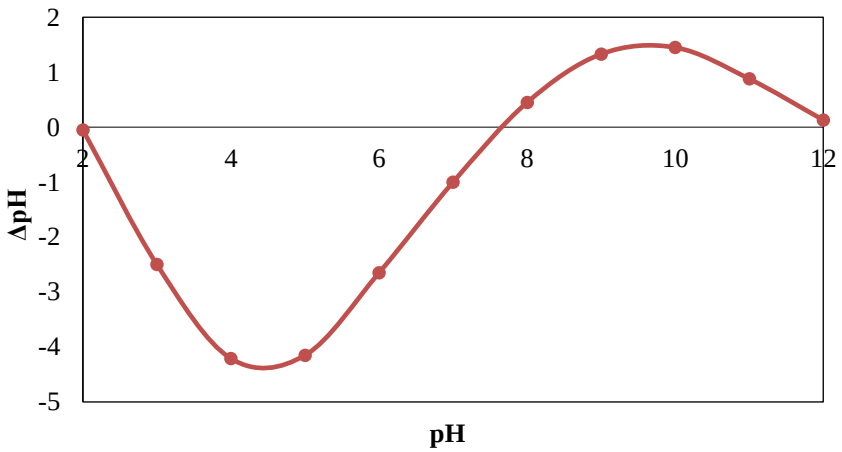

Figure 2. pH zero charge point of activated carbon (pHpzc).

The effect of pH on adsorption performance

pH can condition both the adsorbent's structure and the adsorbent's surface charge. For this, the effect of varying pH on adsorption was examined, employing an initial concentration of 30 mg/L, 0.3 g/L of activated carbon, and a contact duration of 120 minutes. The adsorption removal (%) of FPR onto activated carbon at different pH values is displayed in Figure 3. The best removal

efficiencies were obtained at pHs lower than pH 3. While the removal efficiency was 92% at pH 3, it was 93% at pH 2 and 94% at pH 1.5. When the results were compared by statistical analysis of variance (ANOVA), it was observed that there was no significant difference between the results. The effect of pH on adsorption performance depends on surface charge. As the pH value decreases, the positive charge density on the surface of the adsorbent increases. However, in the study conducted by Arzuoğlu et al. [34], it was revealed that there is no ionization in the structure of FPR at low pH values (1-4). Despite not ionizing, FPR still shows increased adsorption onto the surface of the adsorbent at low pH values. This is attributed to the presence of atoms such as fluorine, nitrogen, and oxygen in the FPR molecule, which have electron pairs available for bonding. These atoms can interact with the positively charged surface of the adsorbent, facilitating the attachment of FPR molecules to the surface. At very low pH values, excess H^+ ions may compete with FPR molecules for the available adsorption sites. However, the adsorption efficiency remained high, suggesting that the favorable interactions between FPR and the activated carbon surface were stronger than the competitive effect of hydrogen ions.

However, a large amount of acid would need to be added to the wastewater to lower the pH of the solution to values lower than 3. Since wastewater is usually discharged in the neutral pH range, and pH 3 can be reached by adding a little acid, pH 3 was chosen for further experiments.

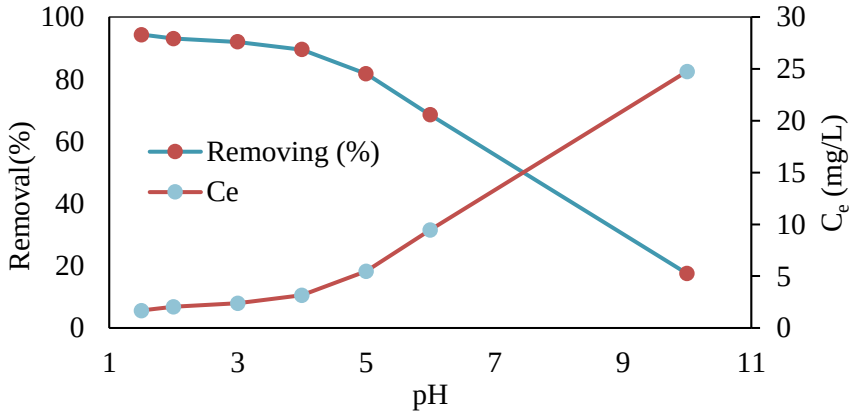

Figure 3. The effect of pH on FPR Adsorption.

The effect of adsorbent dose on adsorption performance

To investigate the impact of varying adsorbent quantities on the adsorption of FPR, experiments were conducted using an initial FPR concentration of 30 mg/L at pH 3, a temperature of 20 °C, and adsorbent doses ranging from 0.10 to 0.50 g/L. When Figure 4 is examined, it can be seen that the adsorption efficiency increased rapidly from 53.67% to 92.00% from adsorbent dosage 0.10 g/L to 0.30 g/L. Adsorption is fast at the beginning of the process due to the presence of active free sites. Increasing the adsorbent dose increases the adsorption capacity as it provides more surface area, but after a certain point, a saturation point can be observed in the adsorption capacity, meaning that adding more adsorbent dose does not increase the performance [35, 36]. There is not a big difference between 0.30 g/L and 0.50 g/L (99.50%) in the adsorption efficiencies. The use of more than this amount of activated carbon will increase the treatment costs. Therefore, the adsorbent dosage was determined as 0.30 g/L.

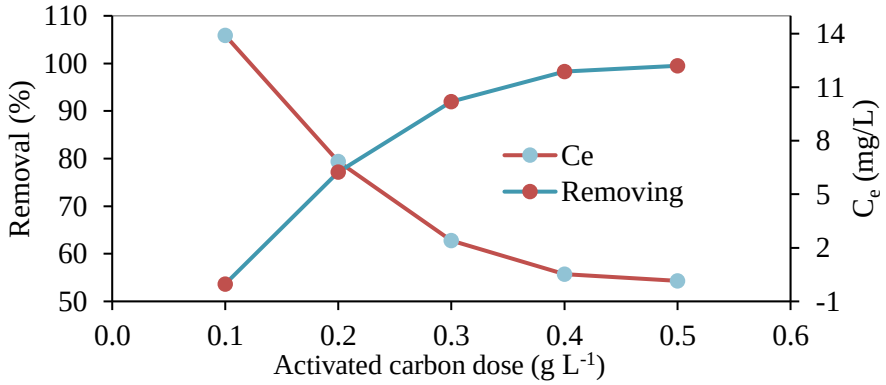

Figure 4. The effect of adsorbent dose on adsorption performance.

The effect of initial concentration on adsorption performance

The effect of initial concentration on adsorption was investigated at pH 3, an adsorbent dose of 0.3 g/L, a temperature of 20 °C, a contact time of 120 min, and initial FPR concentrations ranging from 10 to 50 mg/L. As shown in Figure 5, the FPR removal efficiency decreased slightly from 96.00% to 92.00% when the initial concentration increased from 10 to 30 mg/L. However, a more pronounced decrease from 92.10% to 66.44% was observed when the initial concentration increased from 30 to 50 mg/L. This behavior can be attributed to the progressive saturation of the available adsorption sites on the activated carbon surface. At higher FPR concentrations, the number of molecules competing for a limited number of active sites increases, leading to a reduction in the overall removal efficiency. In addition, intermolecular interactions and steric effects at elevated concentrations may hinder the diffusion of FPR molecules into the porous structure of activated carbon, thereby further decreasing adsorption performance [37, 38].

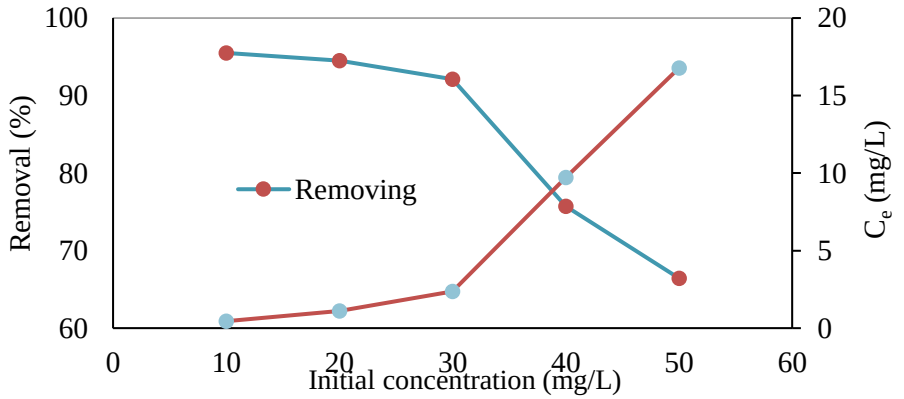

Figure 5. The effect of initial concentration on adsorption performance.

The effect of the contact time on adsorption

In order to determine the interaction time between adsorbate and adsorbent, experiments were carried out at pH 3, 20 °C, 30 mg/L initial concentration, and 0.3 g/L adsorbent dose, and the

results are given in Figure 6. According to this, FPR removal occurs rapidly in the first 15 minutes, continues slightly in the 20 to 90 min range, and is completed in 90 minutes. The FPR concentration gradient formed between the FPR solution and the activated carbon surface created a driving force [39]. This led to a rapid mass transfer, as shown in the figure. The removal efficiency reaches close values starting at 90 minutes and increases from 91.93% to 92.03% at 120 minutes. Statistical analysis (ANOVA, confidence interval 95%) revealed no significant difference in removal times between 90 and 120 minutes. Thus, the best phase contact time for the adsorption process was determined as 120 minutes.

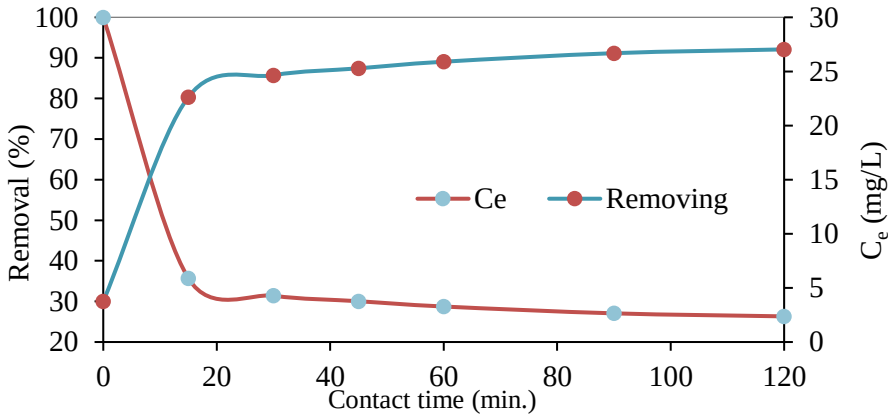

Figure 6. The effect of the contact time on the adsorption performance.

The effect of temperature on adsorption performance

Studies examining the effect of temperature on FPR adsorption were conducted at an initial concentration of 30 mg/L, an adsorbent dose of 0.3 g/ L at pH 3, a contact time of 120 min, and a temperature range of 20-50 °C. As seen in Figure 7, the adsorption rate decreased with increasing temperature, indicating that FPR adsorption is exothermic. Furthermore, the increase in temperature leads to a decrease in the viscosity of the FPR solution. This, in turn, enhances the mobility of FPR molecules, reducing the rate of adsorption onto the activated carbon [40].

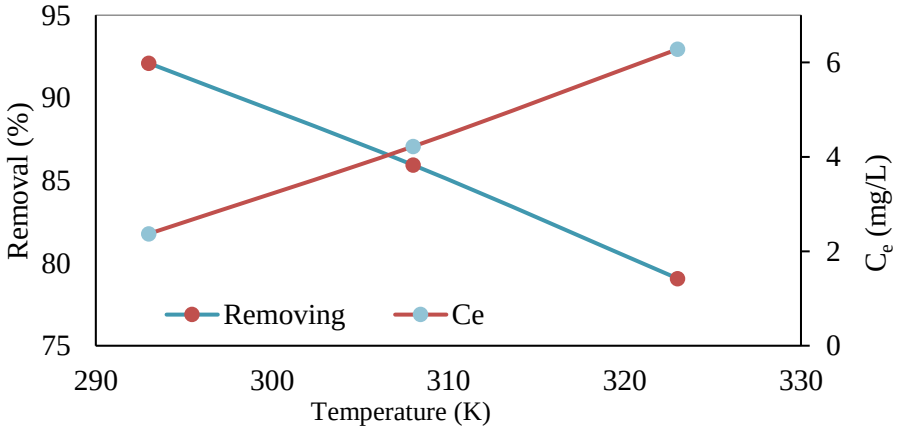

Figure 7. The effect of temperature on the adsorption performance.

Adsorption kinetics

The kinetics of the adsorption process were evaluated using the pseudo-first-order (PFO) and pseudo-second-order (PSO) models, as depicted in Figure 8, and the kinetic parameters and correlation coefficients are presented in Table 1(a). PFO and PSO models are used to express the rate of the adsorption process. The PFO model is based on adsorbent capacity and states that adsorption occurs via diffusion in a boundary layer, while the PSO model assumes that the adsorption rate is controlled by interactions between the adsorbate and the adsorbent surface [41]. As shown in Table 1(a), the correlation coefficient of the PSO model (R^2 = 0.9999) was higher than that of the PFO model (R^2 = 0.9874), indicating that the adsorption of FPR onto activated carbon is best described by the PSO kinetic model. This indicates that the adsorption of FPR molecules on the adsorbent surface is in accordance with the PSO model. At the same time, the fact that the experimentally obtained adsorbed amount (qe=92.00 mg g^{-1}) is very close to the adsorbed amount (qe=94.00 mg g^{-1}) obtained from the PSO rate equation also supports the PSO model. Therefore, the superior fit of the PSO model suggests that the adsorption rate of FPR onto activated carbon was mainly governed by surface-related interactions. However, PSO fitting alone does not provide definitive evidence of chemisorption. In several other investigations concerning antibiotics adsorbed onto activated carbons, it was observed that the PSO model yielded the most accurate fit to the experimental data [42, 43].

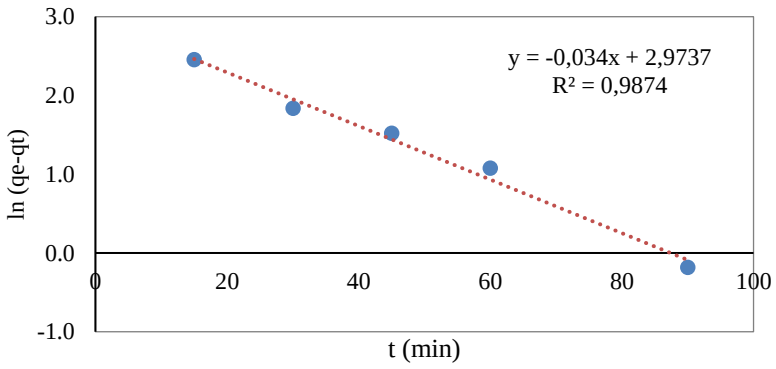

(**A**)

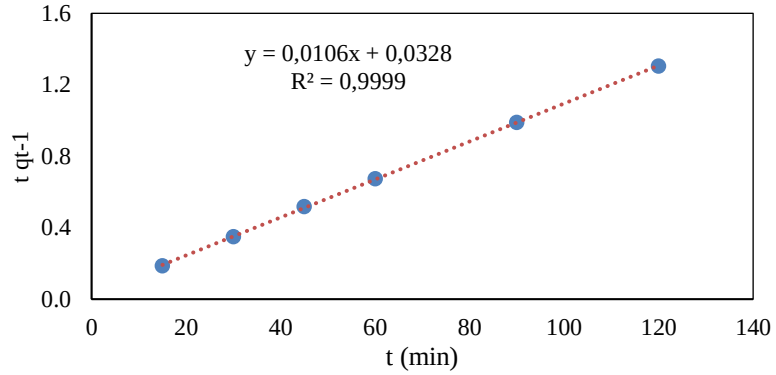

(**B**)

Figure 8. (A) Pseudo-first-order and (B) Pseudo-second-order models (Contact time: 120 min, pH 3, adsorbent dose: 0.30 g/L, initial concentration: 30 mg/L, T: 293 K).

Adsorption isotherm

In the study, we conducted an isotherm analysis to investigate the interaction between FPR and the activated carbon adsorbent. Specifically, we utilized the Langmuir and the Freundlich isotherm models to determine the maximum adsorption capacity and characterize the equilibrium adsorption isotherms. Langmuir and the Freundlich isotherms are given in Figure 9, and the parameters obtained from the Langmuir isotherm model are given in Table 1 (b). The correlation coefficient obtained from the Langmuir isotherm model (R^2 =0.9982) was higher than that obtained from the Freundlich model (R^2 =0.9726). This result indicates that FPR is monolayer adsorbed to a certain number of active centers on the activated carbon adsorbent surface.

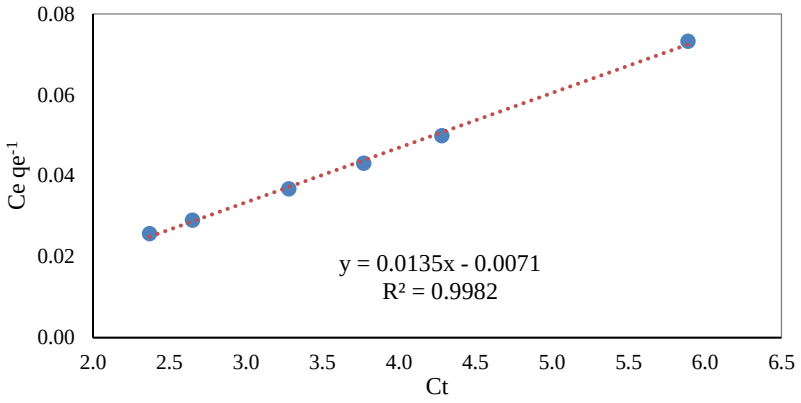

(**A**)

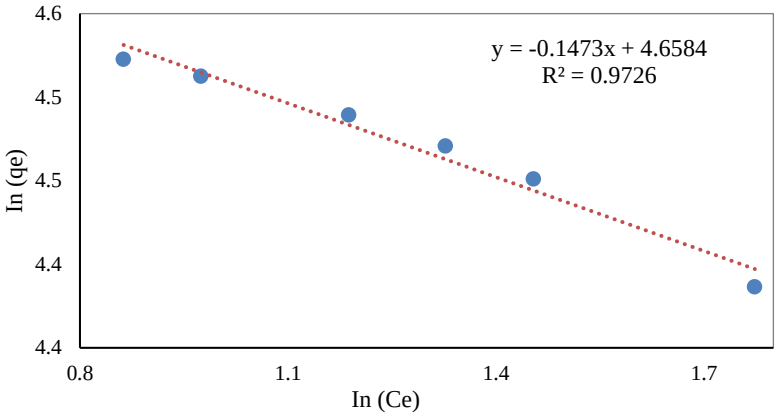

(**B**)

Figure 9. (A) Langmuir and (B) Freundlich isotherms (initial concentration: 30 mg/L, pH: 3, adsorbent dose: 0.30 g/L, contact time: 120 min, T: 293 K).

The R_L constant was calculated as 0.02. The fact that the R_L value is between 0 and 1 shows that the adsorption is suitable for this isotherm. At the same time, the high value of K_L, which expresses the affinity of FPR to activated carbon, in the Langmuir isotherm supports that it is compatible with this isotherm [28].

Thermodynamics of adsorption

Molar Gibbs free energy (ΔG°), enthalpy (ΔH°), and entropy (ΔS°) were calculated with the help of the data obtained from the Van't Hoff plot and are given in Table 1 (c). ΔG^o values are negative, indicating that the adsorption process of FPR on the activated carbon surface occurs spontaneously [44]. The negative ΔH^o (-29.61 kJ mol^{-1}) value indicates that the diffusion and adsorption of FPR on the activated carbon surface is an exothermic process. The ΔH° value of −29.61 kJ mol^{-1} suggests that the adsorption process is predominantly physical in nature [45]. Moreover, the negative value of ΔS^o (-70.77 J mol^{-1} K^{-1}) confirmed the decrease of randomness at the interface of activated carbon and FPR. This decrease in randomness typically occurs because the molecules become more organized and ordered as they adhere to the surface [46].

Table 1. Kinetic parameters (a), isotherm parameters (b), and thermodynamic parameters (c) for the adsorption of favipiravir onto activated carbon.

a) Parameters of the kinetic model for the adsorption process			b) Parameters of isotherm models		
Kinetic model	Parameter	Value	Isotherm Model	Parameter	Value
PFO	k_1 (min^{-1})	0.0340	Langmuir	q_{max} (mg g^{-1})	74.07
	Calculated q_e (mg g^{-1})	19.56		K_L (L mg^{-1})	1.9014
	Experimental q_e (mg g^{-1})	92.00		R_L	0.02
	R^2	0.9874		R^2	0.9982
PSO	k_2 (g mg^{-1} min^{-1})	0.0055	Freundlich	K_F (mg.g^{-1}) (L.mg^{-1})$^{1/n}$	214.70
	Calculated q_e	94.34		n	6.7889
	Experimental q_e (mg g^{-1})	92.00		R^2	0.9726
	R^2	0.9999			

c)Thermodynamic parameters of the adsorption process					
Parameters	ΔG^o (kJ mol^{-1})			ΔH^o (kJ mol^{-1})	ΔS^o (J $mol^{-1}K^{-1}$)
Temperature (K)	293	308	323		
	- 8.873	-7.811	-6.750	-29.61	-70.77

CONCLUSIONS

The aim of this study was to remove the antiviral FPR from synthetic wastewater. After investigating the adsorption processes of this pharmaceutical product by commercial activated carbon, the adsorption process was shown to be an effective method for the removal of FPR contaminated wastewater. Under optimum operating conditions (C_0: 30 mg/L, temperature: 20 °C, pH 3, adsorbent dose: 0.30 g/L, contact time: 120 min.), the adsorption efficiency was determined as 91.93%. The developed process has the capacity to remove most of the FPR discharged to domestic and hospital wastewater at the source. Langmuir isotherm and pseudo-second-order kinetic models are in agreement with our experimental data. Our thermodynamic studies showed that the adsorption of FPR onto activated carbon is spontaneous, exothermic, and predominantly governed by physical interactions. The developed process is shown to be effectively applicable for the treatment of FPR-containing waters such as hospital wastewater and pharmaceutical industrial wastewater.

Credit authorship contribution statement

Nazan Yılmaz: Writing – original draft, Data curation, Supervision, Methodology, Investigation. Oğuzhan Alagöz: Supervision, Investigation, Validation, Resources, Writing. İbrahim Bulduk: Methodology, Writing, Conceptualization.

Declaration of competing interest

The authors declare that they have no conflict of interest in the publication of the manuscript.

ACKNOWLEDGMENTS

We thank the Afyon Kocatepe University Department of Chemical Engineering for its support. We thank Ayşen Nur Durgun for her support during this work.

Data availability

Data will be made available on request.

REFERENCES

1. Couto, C.F.; Lange, L.C.; Amaral, M.C. Occurrence, fate and removal of pharmaceutically active compounds (PhACs) in water and wastewater treatment plants – A review. *J. Water Process Eng.* **2019**, 32,100927.
2. Bilal, M.; Rizwan, K.; Adeel, M.; Iqbal, H.M. Hydrogen-based catalyst-assisted advanced oxidation processes to mitigate emerging pharmaceutical contaminants. *Int. J. Hydrogen Energy* **2022**, 47, 19555-19569.
3. Krasucka, P.; Rombel, A.; Yang, X.J.; Rakowska, M.; Xing, B.; Oleszczuk, P. Adsorption and desorption of antiviral drugs (ritonavir and lopinavir) on sewage sludges as a potential environmental risk. *J. Hazard. Mater.* **2022**, 425, 127901.
4. Yao, L.; Chen, Z.Y.; Dou, W.Y.; Yao, Z.K.; Duan, X.C.; Chen, Z.F.; Ying, G.G. Occurrence, removal and mass loads of antiviral drugs in seven wastewater treatment plants with various treatment processes. *Water Res.* **2021**, 207, 117803.
5. Nannou, C; Ofrydopoulou, A.; Evgenidou, E.; Heath, D.; Heath, E.; Lambropoulou, D. Antiviral drugs in aquatic environment and wastewater treatment plants: A review on occurrence, fate, removal and ecotoxicity. *Sci. Total Environ*. **2020**, 699, 134322.
6. Yao, L.; Dou, W.Y.; Ma, Y.F.; Liu, Y.S. Development and validation of sensitive methods for simultaneous determination of nine antiviral drugs in various environmental matrices by UPLC–MS/MS. *Chemosphere* **2021**, 282, 131047.
7. Silva, M.; Baltrus, J.P.; Williams, C.; Knopf, A.; Zhang, L.; Baltrusaitis, J. Heterogeneous photo-Fenton-like degradation of emerging pharmaceutical contaminants in wastewater using Cu-doped MgO nanoparticles. *Appl. Catal. A: Gen*. **2022**, 630, 118468.
8. Nippes, R.P.; Macruz, P.D.; da Silva, G.N.; Scaliante, M.H.N.O. A critical review on environmental presence of pharmaceutical drugs tested for the COVID-19 treatment. *Process Saf. Environ. Prot*. **2021**, 152, 568-582.
9. Jain, S.; Kumar, P.; Vyas, R.K.; Pandit, P.; Dalai, A.K. Occurrence and removal of antiviral drugs in environment: A review. *Water Air Soil Pollut.* **2013**, 224, 1-19.
10. Barceló, D. An environmental and health perspective for COVID-19 outbreak: Meteorology and air quality influence, sewage epidemiology indicator, hospitals disinfection, drug therapies and recommendations. *J. Environ. Chem. Eng.* **2020**, 8, 104007.

11. Kumari, M.; Kumar, A. Can pharmaceutical drugs used to treat COVID-19 infection lead to human health risk? A hypothetical study to identify potential risk. *Sci. Total Environ.* **2021**, 778, 146303.
12. Kumari, M.; Kumar, A. Environmental and human health risk assessment of mixture of COVID-19 treating pharmaceutical drugs in environmental waters. *Sci. Total Environ.* **2022**, 812, 152485.
13. Nannou, C.; Ofrydopoulou, A.; Evgenidou, E.; Heath, D.; Heath, E.; Lambropoulou, D. Analytical strategies for the determination of antiviral drugs in the aquatic environment. *Trends Environ. Anal. Chem.* **2019**, 24, e00071.
14. Vora, A.; Tiwaskar, M. Favipiravir. *J. Assoc. Physicians India*. **2020**, 68, 91-92.
15. Alamer, A.; Alrashed, A.A.; Alfaifi, M.; Alosaimi, B.; AlHassar, F.; Almutairi, M.; Almulhim, A.S. Effectiveness and safety of favipiravir compared to supportive care in moderately to critically ill COVID-19 patients: A retrospective study with propensity score matching sensitivity analysis. *Curr. Med. Res. Opin.* **2021**, 37,1085-1097.
16. Almoosa, Z.; Saad, M.; Qara, S.; Mustafa, M.; Mansour, A.; Alshab, D.; Al Mutair, A. Favipiravir versus standard of care in patients with severe COVID-19 infections: a retrospective comparative study. *J. Infect. Public Health* **2021**,14, 1247-1253.
17. Deng, W.; Yang, C.; Yang, S.; Chen, H.; Qiu, Z.; Chen, J. Evaluation of favipiravir in the treatment of COVID-19 based on the real world. *Expert Rev. Anti Infect. Ther.* **2022,** 20, 555-565.
18. Saadat, S.; Rawtani, D.; Hussain, C.M. Environmental perspective of COVID-19. *Sci. Total Environ.* **2020**, 728, 138870.
19. Ibáñez, M.; Borova, V.; Boix, C.; Aalizadeh, R.; Bade, R.; Thomaidis, N. S.; Hernández, F. UHPLC-QTOF MS screening of pharmaceuticals and their metabolites in treated wastewater samples from Athens. *J. Hazard. Mater.* **2017**, 323, 26-35.
20. Hassanipour, S.; Arab-Zozani, M.; Amani, B.; Heidarzad, F.; Fathalipour, M.; Martinez-de-Hoyo, R. The efficacy and safety of favipiravir in treatment of COVID-19: a systematic review and meta-analysis of clinical trials. *Sci. Rep.* **2021**, 11, 11022.
21. Gupta, V.K. Application of low-cost adsorbents for dye removal – a review. *J. Environ. Manage.* **2009**, 90, 2313-2342.
22. Yılmaz, N.; Alagöz, O.; Bulduk, İ.; Yıldız, A. Efficient removal of cytotoxic sunitinib from aqueous media using natural bentonite: Adsorption, kinetics, thermodynamics. *Sep. Sci. Technol.* **2026**, 61, 1009-1027.
23. Mengistie, A.A.; Rao, T. S.; Singanan, M. Removal of lead(II) ions from aqueous solutions using activated carbon from *Militia ferruginea* plant leaves. *Bull. Chem. Soc. Ethiop.* **2008**, 22, 349-360.
24. Cuerda-Correa, E.M.; Domínguez-Vargas, J.R.; Olivares-Marín, F.J.; de Heredia, J.B. On the use of carbon blacks as potential low-cost adsorbents for the removal of non-steroidal anti-inflammatory drugs from river water. *J. Hazard. Mater.* **2010**,177, 1046-1053.
25. Paşa, S.; Yılmaz, N.; Bulduk, İ.; Alagöz, O. Effective adsorption performance of hemp root-derived activated carbon for tamoxifen-contaminated wastewater. *J. Mol. Liq.* **2025**, 425, 127219.
26. Imanipoor, J.; Mohammadi, M.; Dinari, M.; Ehsani, M.R. Adsorption and desorption of amoxicillin antibiotic from water matrices using an effective and recyclable MIL-53(Al) metal–organic framework adsorbent. *J. Chem. Eng. Data* **2020**, 66, 389-403.
27. Hassanzadeh-Afruzi, F.; Heidari, G.; Maleki, A. Magnetic nanocomposite hydrogel based on Arabic gum for remediation of lead(II) from contaminated water. *Mater. Chem. Horiz.* **2022**, 1, 107-122.
28. Zaidi, R.; Khan, S. U.; Farooqi, I. H.; Azam, A. Investigation of kinetics and adsorption isotherm for fluoride removal from aqueous solutions using mesoporous cerium–aluminum binary oxide nanomaterials. *RSC Adv.* **2021**, 11, 28744-28760.

29. Ibikunle, A.; Osobamiro, T.; Babarinde, N.; Adaramola, F. Adsorptive sequestration of methylene blue dye from aqueous solution using novel *Roystonea regia* fruit pericarp: İsotherm, kinetics, and thermodynamics. *Gazi Univ. J. Sci.* **2024**, 37, 813-838.
30. Zhang, J.; Lu, F.; He, X.; Liao, Y.; Chen, R.; Xia, R.; Yu, J. The adsorption of biogenetic odorants onto activated carbon: adsorption characteristics and impacts of algal organic matter. *Environ. Res.* **2023**, 238, 117072.
31. Appendix F: Guidelines for standard methods performance requirements. *Official Methods of Analysis of AOAC International* **2016**, 1-18.
32. Azam, K.; Shezad, N.; Shafiq, I.; Akhter, P.; Akhtar, F.; Jamil, F.; Hussain, M. A review on activated carbon modifications for the treatment of wastewater containing anionic dyes. *Chemosphere* **2022**, 306, 135566.
33. Zaher, A.; Taha, M.; Mahmoud, R.K. Possible adsorption mechanisms of the removal of tetracycline from water by La-doped Zn–Fe-layered double hydroxide. *J. Mol. Liq.* **2021**, 322, 114546.
34. Arzuoğlu, Ü.A.; Konçe, İ.; Demiralay, E.Ç. Determination of the ionization constant value of favipiravir in water–acetonitrile binary mixtures and comparison of two different C18 columns. *Süleyman Demirel Univ. Fac. Arts Sci. J. Sci.* **2023**, 18, 129-139.
35. Wu, H.; Wen, Q.; Hu, L.; Gong, M. Effect of adsorbate concentration to adsorbent dosage ratio on the sorption of heavy metals on soils. *J. Environ. Eng.* **2018**, 144, 04017094.
36. Hashem, A.; Aniagor, C.O.; Farag, S.; Fikry, M.; Aly, A.A.; Amr, A. Evaluation of the adsorption capacity of surfactant-modified biomass in an aqueous acid blue 193 system. *Waste Manag. Bull.* **2024**, 2, 172-183.
37. Rápó, E.; Tonk, S. Factors affecting synthetic dye adsorption; desorption studies: A review of results from the last five years (2017–2021). *Molecules* **2021**, 26, 5419.
38. Zhang, Y.; Cheng, L.; Ji, Y. A novel amorphous porous biochar for adsorption of antibiotics: adsorption mechanism analysis via experiment coupled with theoretical calculations. *Chem. Eng. Res. Des.* **2022**, 186, 362-373.
39. Ramadhani, E.D.; Kurniawati, D. Effect of contact time and agitation speed on the adsorption process of methylene blue dyes using longan shell (*Euphoria longan* L.) as biosorbent. *Am. J. Sci. Eng. Res.* **2021**, 4, 143-149.
40. Budnyak, T.M.; Błachnio, M.; Slabon, A.; Jaworski, A.; Tertykh, V.A.; Deryło-Marczewska, A.; Marczewski, A.W. Chitosan deposited onto fumed silica surface as sustainable hybrid biosorbent for Acid Orange 8 dye capture: effect of temperature in adsorption equilibrium and kinetics. *J. Phys. Chem. C* **2020**, 124, 15312-15323.
41. Bullen, J.C.; Saleesongsom, S.; Gallagher, K.; Weiss, D.J. A revised pseudo-second-order kinetic model for adsorption, sensitive to changes in adsorbate and adsorbent concentrations. *Langmuir* **2021**, 37, 3189-3201.
42. Pezoti, O.; Cazetta, A.L.; Bedin, K.C.; Souza, L.S.; Martins, A.C.; Silva, T.L.; Santos Júnior, O.O.; Visentainer, J.V.; Almeida, V.C. NaOH-activated carbon of high surface area produced from guava seeds as a high-efficiency adsorbent for amoxicillin removal: Kinetic, isotherm and thermodynamic studies. *Chem. Eng. J.* **2016**, 288, 778-788.
43. Shankar, S.N.; Dinakaran, D.R.; Chandran, D.K.; Mantha, G.; Srinivasan, B.; Kannaian, U.P.N. Adsorption kinetics, equilibrium and thermodynamics of a textile dye V5BN by a natural nanocomplex material: clinoptilolite. *Energy Nexus* **2023**, 10, 100197.
44. Alvarez-Galvan, Y.; Minofar, B.; Futera, Z.; Francoeur, M.; Jean-Marius, C.; Brehm, N.; Yacou, C.; Jauregui-Haza, J.; Gaspard, S. Adsorption of hexavalent chromium using activated carbon produced from *Sargassum* ssp.: comparison between lab experiments and molecular dynamics simulations. *Molecules* **2022**, 27, 6040.
45. Hellal, M.S.; Rashad, A.M.; Kadimpati, K.K.; Attia, S.K.; Fawzy, M.E. Adsorption characteristics of nickel(II) from aqueous solutions by zeolite socony mobile-5 (ZSM-5) incorporated in sodium alginate beads. *Sci. Rep.* **2023**, 13, 19601.